Optical absorption spectra, crystal-field energy levels and intensities of Eu^{3+} in $GdAl_3(BO_3)_4$

1994 J. Phys.: Condens. Matter 6 7797

(http://iopscience.iop.org/0953-8984/6/38/017)

J. Phys.: Condens. Matter 6 (1994) 7797–7812. Printed in the UK

Optical absorption spectra, crystal-field energy levels and intensities of Eu^{3+} in $GdAl_3(BO_3)_4$

C Görller-Walrand, E Huygen, K Binnemans and L Fluyt

University of Leuven, Laboratory of Inorganic Chemistry, Celestijnenlaan 200F, B-3001 Heverlee, Belgium

Received 4 March 1994, in final form 6 May 1994

Abstract. Locations and assignments of crystal-field levels in polarized absorption spectra (77 and 298 K) are reported for Eu^{3+} in the $GdAl_3(BO_3)_4$ huntite matrix. The levels are analysed in terms of 20 free-ion and six crystal-field parameters (D_3 symmetry). J mixing is taken into account. The influence of a parameter change on the calculated energy levels is discussed and it is shown that some parameters affect only particular levels. Spectral intensities of the 4f–4f transitions are given and parametrized using a set of $B_{\lambda kq}$ intensity parameters.

1. Introduction

The crystal structure of $GdAl_3(BO_3)_4$ doped with Eu^{3+} is reported by Kuroda *et al* [1]. The host lattice is isostructural with the mineral huntite, $CaMg_3(CO_3)_4$. There is only one crystallographic site available for the lanthanide ions. Eu^{3+} is surrounded by six oxygens and the coordination polyhedron is a distorted trigonal prism. Because the upper triangle is twisted over an angle ϕ with regard to the lower triangle, the site symmetry is lowered by this distortion from D_{3h} to D_3. The first spectroscopic data of Eu^{3+} in $GdAl_3(BO_3)_4$ (polarized emission spectra) have been published by Lagerwey and Blasse [2]. They found that the $^5D_0 \rightarrow {}^7F_1$ transition is strongly polarized, whereas the $^5D_2 \rightarrow {}^7F_0$ transition is unpolarized. The authors consider the latter transition as a pseudoquadrupole transition. Their work has been repeated by Peacock [3], but this author finds that the $^5D_2 \rightarrow {}^7F_0$ transition is polarized according to the selection rules for induced electric dipole transitions in a D_3 symmetry. He also published the axial and polarized absorption spectra of the $^5D_1 \leftarrow {}^7F_0$ and $^5D_2 \leftarrow {}^7F_0$ transitions. The intensities of the $^5D_1 \leftarrow {}^7F_0$, $^5D_2 \leftarrow {}^7F_0$, $^5D_0 \leftarrow {}^7F_1$ and $^5D_1 \leftarrow {}^7F_1$ transitions are discussed by Kuroda *et al* [1] in the framework of anisotropic ligand polarization contributions to the transition probabilities in Eu^{3+}. Kellendonk and Blasse [4] have reported the emission and excitation spectra of the Eu^{3+} luminescence and energy transfer phenomena in $Gd_{1-x}Eu_xAl_3(BO_3)_4$ ($0 < x \leqslant 1$). The position of the energy levels between 0 and 19 000 cm^{-1} of Eu^{3+} in $EuAl_3(BO_3)_4$ are given. The axial absorption, polarized absorption, fluorescence and magnetic circular dichroism (MCD) spectra of Eu^{3+}-doped $YAl_3(BO_3)_4$ have been published by Görller-Walrand *et al* [5–7].

In this paper we report the polarized absorption spectra of Eu^{3+}-doped $GdAl_3(BO_3)_4$ between 16 000 and 32 000 cm^{-1} at 77 and 298 K. The data are analysed using a parametric Hamiltonian with a total of 26 parameters. The influence of a parameter change on the calculated energy levels is considered. It will be shown that a change does not have a similar effect on each level. The dipole strengths of the 4f–4f transitions in Eu^{3+} are given

0953-8984/94/387797+16$19.50

and parametrized, on the basis of the anisotropic ligand polarization model proposed by Mason *et al* [8], and adapted by Reid and Richardson [9–11].

2. Experimental details

The Eu^{3+}-doped $GdAl_3(BO_3)_4$ crystals were kindly donated by Professor G Blasse of Utrecht University (The Netherlands). Optical absorption spectra were recorded using an AVIV 17DS spectrophotometer. In the visible and UV regions, the instrument has a wavelength resolution better than 0.1 nm. The wavelength accuracy is ±0.4 nm. Light polarization is achieved by a Glan–Thompson polarizer. For low-temperature measurements, the sample is cooled in an optical dewar (Oxford Instruments) filled with liquid nitrogen (77 K).

3. Selection rules

The crystal-field levels are assigned in a D_3 symmetry and they have the symmetry labels Γ_1, Γ_2 and Γ_3, according to the Koster notations [12]. The assignments are based on the polarization characteristics of the transitions and the selection rules for induced electric dipole (ED) and magnetic dipole (MD) transitions (table 1); α, σ and π are defined in the usual manner as

α spectrum: $\boldsymbol{c} \| z$

σ spectrum: $\boldsymbol{c} \perp z, \boldsymbol{H} \| \boldsymbol{c}$

π spectrum: $\boldsymbol{c} \perp z, \boldsymbol{E} \| \boldsymbol{c}$

z is the propagation direction of the light, $\boldsymbol{c}$ is the main crystal axis, and $\boldsymbol{E}$ and $\boldsymbol{H}$ are the electric and magnetic field vectors of the incident light respectively.

Table 1. Selection rules for induced electric dipole (ED) and magnetic dipole (MD) transitions in a D_3 symmetry.

	ED			MD		
	Γ_1	Γ_2	Γ_3	Γ_1	Γ_2	Γ_3
Γ_1	—	π	α, σ	—	σ	α, π
Γ_2	π	—	α, σ	σ	—	α, π
Γ_3	α, σ	α, σ	α, σ, π	α, π	α, π	α, π, σ

The ground state of Eu^{3+} is $^7F_0$ and it has symmetry label Γ_1. Because no $\Gamma_1 \leftarrow \Gamma_1$ transitions are allowed by the selection rules, transitions starting from $^7F_0$ are not suitable for detecting crystal-field levels with Γ_1 symmetry. These levels can be located with the aid of transitions starting from the $^7F_1$ multiplet (which has crystal-field levels with Γ_2 and Γ_3 symmetry).

4. Analysis of the polarized spectra

4.1. $^5D_0 \leftarrow {}^7F_{0,1,2}$

Transitions to $^5D_0$ are found between 16 000 and 17 000 cm^{-1}.

The $^5D_0 \leftarrow {}^7F_0$ transition is symmetry-forbidden for both ED and MD transitions ($\Gamma_1 \leftarrow \Gamma_1$) and is not observed in the spectra.

For $^5D_0 \leftarrow {}^7F_1$, two absorption peaks are observed, one in σ polarization at 16 787 cm^{-1} ($\Gamma_1 \leftarrow \Gamma_2$) and another in both α and π polarization at 16 915 cm^{-1} ($\Gamma_1 \leftarrow \Gamma_3$). According to the selection rules, it is a MD transition. The energy difference between the Γ_3 and the Γ_2 levels of $^7F_1$ is 128 cm^{-1}.

The $^5D_0 \leftarrow {}^7F_2$ transition shows two absorption peaks in the α and σ spectrum: 16 184 cm^{-1} ($\Gamma_1 \leftarrow \Gamma_3^b$) and 16 305 cm^{-1} ($\Gamma_1 \leftarrow \Gamma_3^a$). No peaks are observed in the π spectrum. This transition has an ED character. The energy gap between the two Γ_3 levels of the $^7F_2$ multiplet is 121 cm^{-1}.

4.2. $^5D_1 \leftarrow {}^7F_{0,1,2}$

These transitions can be found in the spectrum between 17 900 and 19 100 cm^{-1}.

The $^5D_1 \leftarrow {}^7F_0$ transition shows two peaks in the spectrum, one in both α and π polarization at 19 000 cm^{-1} ($\Gamma_3 \leftarrow \Gamma_1$) and one in σ polarization at 19 030 cm^{-1} ($\Gamma_2 \leftarrow \Gamma_1$). This transition is analogous to the $^5D_0 \leftarrow {}^7F_1$ transition and also has a MD nature. The energy difference between the two crystal-field levels of the $^5D_1$ multiplet (Γ_2 and Γ_3) is 30 cm^{-1}.

For the $^5D_1 \leftarrow {}^7F_1$ three peaks are detected in the α and σ spectrum: 18 539 cm^{-1} ($\Gamma_3 \leftarrow \Gamma_2$), 18 667 cm^{-1} ($\Gamma_3 \leftarrow \Gamma_3$) and 18 700 cm^{-1} ($\Gamma_2 \leftarrow \Gamma_3$). The π spectrum shows no signals. Although $\Delta J = 0$, $^5D_1 \leftarrow {}^7F_1$ is a MD transition according to the selection rules. With the knowledge of the position of the $^5D_1$ crystal-field levels from $^5D_1 \leftarrow {}^7F_0$, the crystal-field levels of $^7F_1$ can be determined from the $^5D_1 \leftarrow {}^7F_1$ transition: Γ_3 at 331 cm^{-1} and Γ_2 at 461 cm^{-1}. The $^5D_0$ level can be placed at 17 245 cm^{-1}.

The $^5D_1 \leftarrow {}^7F_2$ signals are very weak, and only peaks in σ polarization can be assigned without ambiguity: 17 938 cm^{-1} ($\Gamma_3 \leftarrow \Gamma_3^b$), 17 969 cm^{-1} ($\Gamma_2 \leftarrow \Gamma_3^b$), 18 058 cm^{-1} ($\Gamma_3 \leftarrow \Gamma_3^a$) and 18 090 cm^{-1} ($\Gamma_2 \leftarrow \Gamma_3^a$). These transitions make it possible to find the energy of some crystal-field levels of $^7F_2$: Γ_3^a at 940 cm^{-1} and Γ_3^b at 1061 cm^{-1}. The position of the Γ_1 level cannot be determined until now.

4.3. $^5D_2 \leftarrow {}^7F_{0,1,2}$

Transitions to the $^5D_2$ level are present in the spectrum between 20 000 and 21 600 cm^{-1}.

Two peaks in the α and σ spectrum belong to $^5D_2 \leftarrow {}^7F_0$: one at 21 461 cm^{-1} ($\Gamma_3^a \leftarrow \Gamma_1$) and another at 21 531 cm^{-1} ($\Gamma_3^b \leftarrow \Gamma_1$). No peaks are seen in π polarization. The transition has an ED character.

The transitions from $^7F_1$ to $^5D_2$ give four peaks in the σ spectrum: 21 000 cm^{-1} ($\Gamma_3^a \leftarrow \Gamma_2$), 21 071 cm^{-1} ($\Gamma_3^b \leftarrow \Gamma_2$), 21 130 cm^{-1} ($\Gamma_3^a \leftarrow \Gamma_3$) and 21 201 cm^{-1} ($\Gamma_3^b \leftarrow \Gamma_3$). The π spectrum shows no clear signals.

The $^5D_2 \leftarrow {}^7F_2$ transition gives a single peak in π polarization at 20 521 cm^{-1} ($\Gamma_3^a \leftarrow \Gamma_3^a$). Three signals are detected in the σ spectrum at 20 381 cm^{-1} ($\Gamma_1 \leftarrow \Gamma_3^b$) and at 20 501 cm^{-1} ($\Gamma_1 \leftarrow \Gamma_3^a$). The third peak at 20 241 cm^{-1} cannot be assigned unambiguously.

4.4. $^5D_3 \leftarrow {}^7F_{0,1}$

Transitions to $^5D_3$ are detected between 23 900 and 24 550 cm^{-1}. In π polarization, two peaks can be assigned: one at 24 327 cm^{-1} ($\Gamma_2^a \leftarrow \Gamma_1$) and one at 24 420 cm^{-1} ($\Gamma_2^b \leftarrow \Gamma_1$). The σ spectrum shows one peak at 24 357 cm^{-1} ($\Gamma_3^a \leftarrow \Gamma_1$).

The three signals of the $^5D_3 \leftarrow {}^7F_1$ transition can be assigned as follows: 23 946 cm^{-1} ($\Gamma_1 \leftarrow \Gamma_2$), 24 000 cm^{-1} ($\Gamma_3^a \leftarrow \Gamma_3$) and 24 020 cm^{-1} ($\Gamma_3^b \leftarrow \Gamma_3$). The absorption peak at 24 022 cm^{-1} in both α and σ spectra is the $\Gamma_2^a \leftarrow \Gamma_3$ transition and the peak at 24 075 cm^{-1} is the $\Gamma_2^b \leftarrow \Gamma_3$ one.

4.5. $^5L_6 \leftarrow {}^7F_{0,1}$

Transitions to $^5L_6$ are seen between 24 500 and 25 500 cm^{-1}. Because of the large splitting of the $^5L_6$ manifold (nearly 500 cm^{-1}), transitions from $^7F_0$ to the lowest crystal-field levels of $^5L_6$ are found in the same region as the transitions from $^7F_1$ to the highest crystal-field levels of $^5L_6$. This ambiguity can be removed by recording spectra at 77 K, so that the thermal population of the $^7F_1$ crystal-field levels is very low and only transitions starting from the ground state $^7F_0$ are detected.

For the $^5L_6 \leftarrow {}^7F_0$ transition, four peaks are predicted theoretically in α and σ polarization and two peaks in π polarization. The two peaks in π signals are indeed found: one at 24 903 cm^{-1} ($\Gamma_2^a \leftarrow \Gamma_1$) and one at 25 231 cm^{-1} ($\Gamma_2^b \leftarrow \Gamma_1$). In the α and σ spectrum only three of the four peaks are found: 24 974 cm^{-1} ($\Gamma_3^a \leftarrow \Gamma_1$), 25 052 cm^{-1} ($\Gamma_3^b \leftarrow \Gamma_1$) and 25 367 cm^{-1} ($\Gamma_3^d \leftarrow \Gamma_1$).

Four signals in the α and σ spectra at room temperature and three signals in the π spectrum are assigned to the $^5L_6 \leftarrow {}^7F_1$ transition.

4.6. $^5D_4 \leftarrow {}^7F_{0,1}$

Transitions from $^7F_0$ and $^7F_1$ to the $^5D_4$ level are observed between 27 000 and 27 700 cm^{-1}.

Three signals of the $^5D_4 \leftarrow {}^7F_0$ transition are seen in the σ and α spectrum: 27 574 cm^{-1} ($\Gamma_3^a \leftarrow \Gamma_1$), 27 582 cm^{-1} ($\Gamma_3^b \leftarrow \Gamma_1$) and 27 660 cm^{-1} ($\Gamma_3^c \leftarrow \Gamma_1$). The π spectrum shows two peaks, one at 27 591 cm^{-1} ($\Gamma_2 \leftarrow \Gamma_1$) and another at 27 655 cm^{-1}. It is not possible to assign this transition unequivocally.

Transitions from $^7F_1$ are only found in σ polarization.

4.7. *Transitions to the other multiplets*

The assignments of the signals in the other spectral regions are not possible without the aid of calculated crystal-field levels (see further). A huge number of levels are calculated, but only a limited number of them are effectively found. Moreover, the overlap between the crystal-field levels of different spin–orbit coupling terms is very strong. This is also found for Eu^{3+} in other systems, e.g. EuODA [13] and $LiYF_4$ [14]. Between 26 000 and 29 000 cm^{-1} transitions to the ^5L_J ($J = 7, 8, 9, 10$) and the ^5G_J ($J = 2, 3, 4, 5, 6$) are found, whereas the ^5H_J ($J = 3, 4, 5, 6, 7$) levels are between 29 000 and 32 000 cm^{-1}. Between 32 000 and 33 000 cm^{-1} the Gd^{3+} multiplets $^6P_{7/2}$ and $^6P_{5/2}$ are detected. Over 33 000 cm^{-1}, the 4f–4f transitions are overwhelmed by a broad intense band (charge-transfer band?).

All the observed transitions in the polarized absorption of Eu^{3+}-doped $GdAl_3(BO_3)_4$ are summarized in table 2. The spectra at 298 K are given in figure 1. It is obvious that the absorption peaks are sharp even at this temperature. This is a characteristic feature of the ions in the middle of the lanthanide series (Eu^{3+}, Gd^{3+} and Tb^{3+}).

Table 2. Summary of the transitions in the polarized absorption spectra of Eu^{3+} in $GdAl_3(BO_3)_4$. Assignments are made in a D_3 symmetry.

Transition	Assignment	Energy (cm^{-1})	Polarization	Transition	Assignment	Energy (cm^{-1})	Polarization
$^5D_0 \leftarrow {}^7F_2$	$\Gamma_1 \leftarrow \Gamma_3^b$	16184	$\alpha+\sigma$	$^5L_7 \leftarrow {}^7F_0$,	$\Gamma_3 \leftarrow \Gamma_1$	25956	$\alpha+\sigma$
	$\Gamma_1 \leftarrow \Gamma_3^a$	16305	$\alpha+\sigma$				
				$^5G_2 \leftarrow {}^7F_0$	$\Gamma_2 \leftarrow \Gamma_1$	26025	π
$^5D_0 \leftarrow {}^7F_1$	$\Gamma_1 \leftarrow \Gamma_2$	16787	σ		$\Gamma_3 \leftarrow \Gamma_1$	26051	$\alpha+\sigma$
	$\Gamma_1 \leftarrow \Gamma_3$	16915	$\alpha+\pi$		$\Gamma_3 \leftarrow \Gamma_1$	26093	$\alpha+\sigma$
					$\Gamma_2 \leftarrow \Gamma_1$	26179	π
$^5D_1 \leftarrow {}^7F_2$	$\Gamma_3 \leftarrow \Gamma_3^b$	17938	$\alpha+\sigma$		$\Gamma_3 \leftarrow \Gamma_1$	26227	$\alpha+\sigma$
	$\Gamma_2 \leftarrow \Gamma_3^b$	17969	$\alpha+\sigma$		$\Gamma_3 \leftarrow \Gamma_1$	26272	$\alpha+\sigma$
	$\Gamma_3 \leftarrow \Gamma_3^a$	18058	$\alpha+\sigma$		$\Gamma_2 \leftarrow \Gamma_1$	26288	π
	$\Gamma_2 \leftarrow \Gamma_3^a$	18090	$\alpha+\sigma$		$\Gamma_3 \leftarrow \Gamma_1$	26332	$\alpha+\sigma$
$^5D_1 \leftarrow {}^7F_1$	$\Gamma_3 \leftarrow \Gamma_2$	18539	$\alpha+\sigma$	$^5G_{3,4,5,6} \leftarrow {}^7F_0$	$\Gamma_3 \leftarrow \Gamma_1$	26435	$\alpha+\sigma$
	$\Gamma_3 \leftarrow \Gamma_3$	18667	$\alpha+\sigma$		$\Gamma_2 \leftarrow \Gamma_1$	26433	π
	$\Gamma_2 \leftarrow \Gamma_3$	18700	$\alpha+\sigma$		$\Gamma_3 \leftarrow \Gamma_1$	26455	$\alpha+\sigma$
					$\Gamma_2 \leftarrow \Gamma_1$	26465	π
$^5D_1 \leftarrow {}^7F_0$	$\Gamma_3 \leftarrow \Gamma_1$	19000	$\alpha+\pi$		$\Gamma_3 \leftarrow \Gamma_1$	26484	$\alpha+\sigma$
	$\Gamma_2 \leftarrow \Gamma_1$	19030	σ		$\Gamma_2 \leftarrow \Gamma_1$	26513	π
					$\Gamma_3 \leftarrow \Gamma_1$	26517	$\alpha+\sigma$
$^5D_2 \leftarrow {}^7F_2$	$\Gamma_1 \leftarrow \Gamma_3^b$	20381	σ		$\Gamma_3 \leftarrow \Gamma_1$	26544	$\alpha+\sigma$
	$\Gamma_1 \leftarrow \Gamma_3^a$	20501	σ		$\Gamma_3 \leftarrow \Gamma_1$	26583	$\alpha+\sigma$
	$\Gamma_3^a \leftarrow \Gamma_3^a$	20521	π		$\Gamma_2 \leftarrow \Gamma_1$	26622	π
					$\Gamma_3 \leftarrow \Gamma_1$	26650	$\alpha+\sigma$
$^5D_2 \leftarrow {}^7F_1$	$\Gamma_3^a \leftarrow \Gamma_2$	21000	$\alpha+\sigma$		$\Gamma_3 \leftarrow \Gamma_1$	26717	$\alpha+\sigma$
	$\Gamma_3^b \leftarrow \Gamma_2$	21071	$\alpha+\sigma$		$\Gamma_3 \leftarrow \Gamma_1$	26805	$\alpha+\sigma$
	$\Gamma_3^a \leftarrow \Gamma_3$	21130	$\alpha+\sigma$		$\Gamma_3 \leftarrow \Gamma_1$	26834	$\alpha+\sigma$
	$\Gamma_3^b \leftarrow \Gamma_3$	21201	$\alpha+\sigma$				
				$^5D_4 \leftarrow {}^7F_1$	$\Gamma_3^a \leftarrow \Gamma_2$	27115	σ
$^5D_2 \leftarrow {}^7F_0$	$\Gamma_3^a \leftarrow \Gamma_1$	21461	$\alpha+\sigma$		$\Gamma_3^c \leftarrow \Gamma_2$	27198	σ
	$\Gamma_3^b \leftarrow \Gamma_1$	21531	$\alpha+\sigma$		$\Gamma_3^a \leftarrow \Gamma_3$	27247	σ
					$\Gamma_3^c \leftarrow \Gamma_3$	27320	σ
$^5D_3 \leftarrow {}^7F_1$	$\Gamma_1 \leftarrow \Gamma_2$	23946	π				
	$\Gamma_3^a \leftarrow \Gamma_3$	24000	π	$^5D_4 \leftarrow {}^7F_0$	$\Gamma_3^a \leftarrow \Gamma_1$	27574	$\alpha+\sigma$
	$\Gamma_3^b \leftarrow \Gamma_3$	24020	π		$\Gamma_3^b \leftarrow \Gamma_1$	27582	$\alpha+\sigma$
	$\Gamma_2^a \leftarrow \Gamma_3$	24022	$\alpha+\sigma$		$\Gamma_2 \leftarrow \Gamma_1$	27591	π
	$\Gamma_2^b \leftarrow \Gamma_3$	24075	$\alpha+\sigma$		$\Gamma_1^b \leftarrow \Gamma_1$	27655	π
					$\Gamma_3^c \leftarrow \Gamma_1$	27660	$\alpha+\sigma$
$^5D_3 \leftarrow {}^7F_0$	$\Gamma_2^a \leftarrow \Gamma_1$	24327	π				
	$\Gamma_3 \leftarrow \Gamma_1$	24357	σ	$^5H_J \leftarrow {}^7F_0$	$\Gamma_3 \leftarrow \Gamma_1$	30668	$\alpha+\sigma$
	$\Gamma_3^b \leftarrow \Gamma_1$	24420	π		$\Gamma_2 \leftarrow \Gamma_1$	30712	π
					$\Gamma_2 \leftarrow \Gamma_1$	30824	π
$^5L_6 \leftarrow {}^7F_1$	$\Gamma_1 \leftarrow \Gamma_2$	24514	π		$\Gamma_3 \leftarrow \Gamma_1$	30865	$\alpha+\sigma$
	$\Gamma_2^a \leftarrow \Gamma_2$	24523	$\alpha+\sigma$		$\Gamma_2 \leftarrow \Gamma_1$	30973	π
	$\Gamma_2^a \leftarrow \Gamma_3$	24570	$\alpha+\sigma$		$\Gamma_2 \leftarrow \Gamma_1$	31012	π
	$\Gamma_3^a \leftarrow \Gamma_3$	24634	$\alpha+\sigma$		$\Gamma_3 \leftarrow \Gamma_1$	31103	$\alpha+\sigma$
	$\Gamma_3^b \leftarrow \Gamma_3$	24723	$\alpha+\sigma$		$\Gamma_3 \leftarrow \Gamma_1$	31155	$\alpha+\sigma$
	$\Gamma_3^c \leftarrow \Gamma_3$	24835	π		$\Gamma_2 \leftarrow \Gamma_1$	31156	π
$^5L_6 \leftarrow {}^7F_0$	$\Gamma_2^a \leftarrow \Gamma_1$	24903	π		$\Gamma_2 \leftarrow \Gamma_1$	31190	π
$^5L_6 \leftarrow {}^7F_1$	$\Gamma_2^a \leftarrow \Gamma_2$	24915	$\alpha+\sigma$		$\Gamma_3 \leftarrow \Gamma_1$	31288	$\alpha+\sigma$
$^5L_6 \leftarrow {}^7F_0$	$\Gamma_3^a \leftarrow \Gamma_1$	24974	$\alpha+\sigma$		$\Gamma_3 \leftarrow \Gamma_1$	31327	$\alpha+\sigma$
$^5L_6 \leftarrow {}^7F_1$	$\Gamma_3^a \leftarrow \Gamma_2$	25031	π		$\Gamma_2 \leftarrow \Gamma_1$	31332	π
$^5L_6 \leftarrow {}^7F_0$	$\Gamma_3^b \leftarrow \Gamma_1$	25052	$\alpha+\sigma$		$\Gamma_2 \leftarrow \Gamma_1$	31400	π
	$\Gamma_2^b \leftarrow \Gamma_1$	25231	π		$\Gamma_3 \leftarrow \Gamma_1$	31406	$\alpha+\sigma$
	$\Gamma_3^a \leftarrow \Gamma_1$	25367	$\alpha+\sigma$		$\Gamma_3 \leftarrow \Gamma_1$	31537	$\alpha+\sigma$
					$\Gamma_2 \leftarrow \Gamma_1$	31620	π

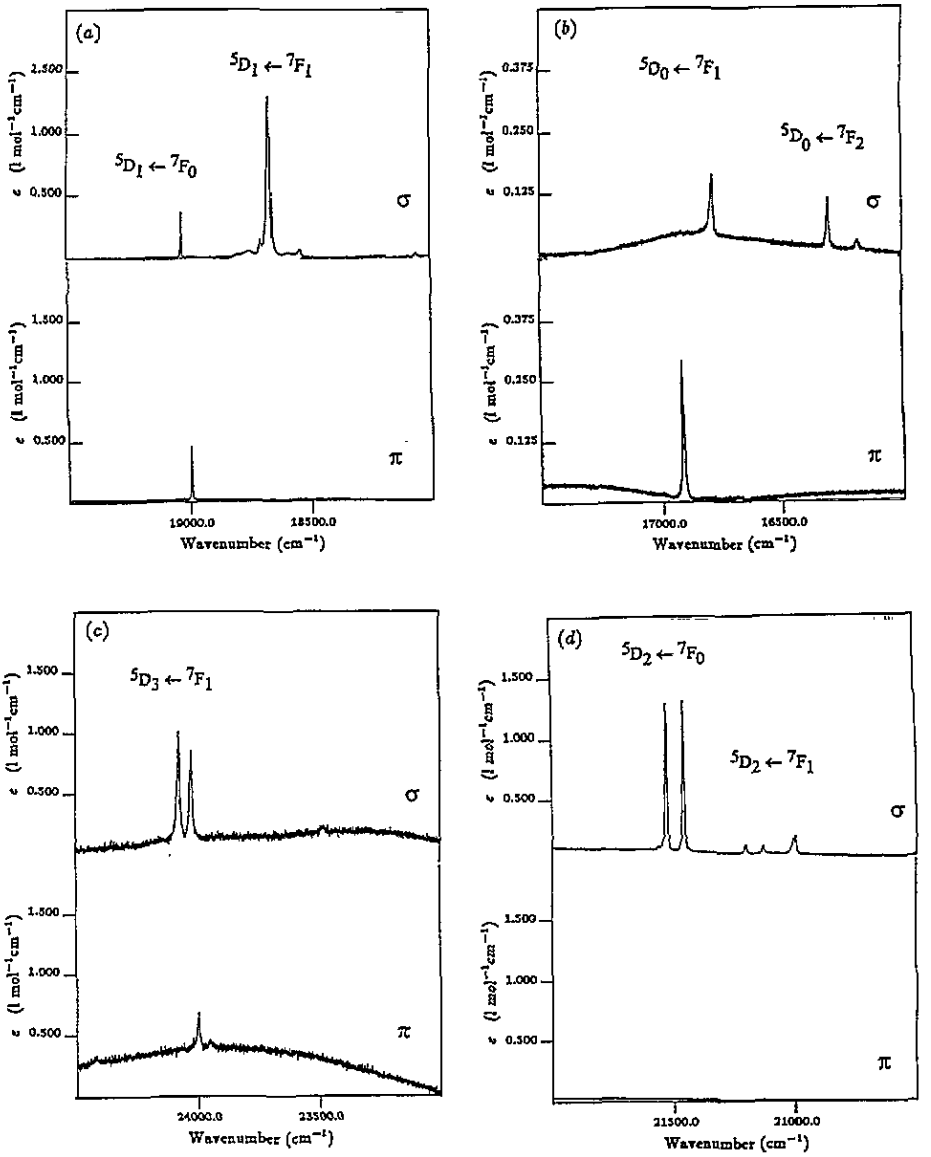

Figure 1. The polarized orthoaxial absorption spectra of Eu^{3+}-doped $GdAl_3(BO_3)_4$ at 298 K: (*a*) $^5D_1 \leftarrow {}^7F_0$, $^5D_1 \leftarrow {}^7F_1$; (*b*) $^5D_0 \leftarrow {}^7F_1$, $^5D_0 \leftarrow {}^7F_2$; (*c*) $^5D_3 \leftarrow {}^7F_1$; (*d*) $^5D_2 \leftarrow {}^7F_0$, $^5D_2 \leftarrow {}^7F_1$; (*e*) $^5G_{3,4,5,6} \leftarrow {}^7F_0$, $^5L_7 \leftarrow {}^7F_0$, $^5G_2 \leftarrow {}^7F_0$; (*f*) $^5L_6 \leftarrow {}^7F_0$, $^5L_6 \leftarrow {}^7F_1$; (*g*) $^5H_{3,4,5,6,7} \leftarrow {}^7F_0$; (*h*) $^5D_4 \leftarrow {}^7F_0$, $^5D_4 \leftarrow {}^7F_1$.

5. Energy level scheme and parametrization

The experimental energy sequence is simulated using a parametric Hamiltonian operation adapted to the f^6 configuration of the Eu^{3+} ion, including intermediate coupling and *J* mixing. The total Hamiltonian can be written as a free-ion part and a crystal-field part:

$$H = H_{\text{free ion}} + H_{\text{crystal field}}. \tag{1}$$

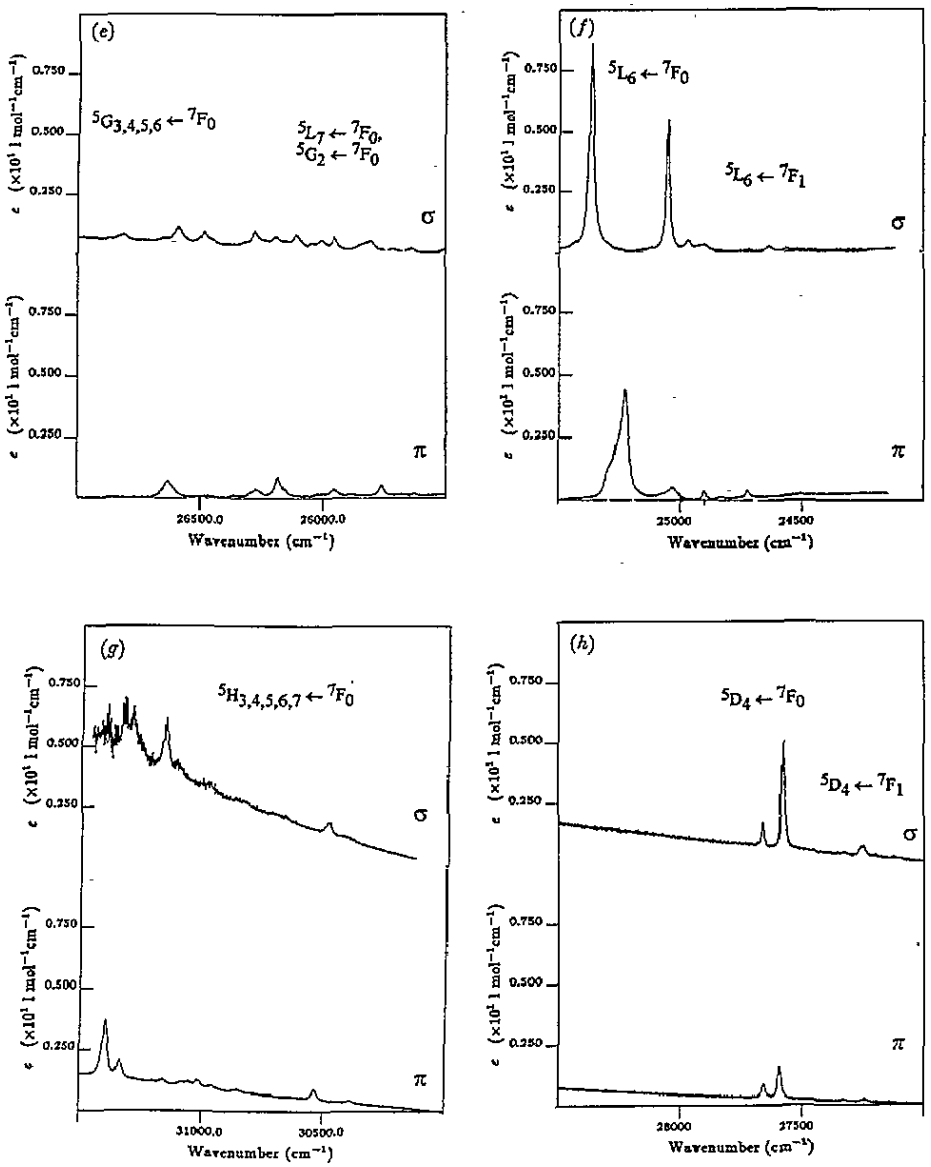

Figure 1. (Continued)

The free-ion Hamiltonian is characterized by a set of three repulsion parameters (F^2, F^4, F^6), by the spin–orbit coupling constant ζ_{4f}, the Trees configuration interaction parameters (α, β, γ), the three-body configuration-interaction parameters (T^2, T^3, T^4, T^6, T^7, T^8) and parameters that describe magnetic interactions (M^0, M^2, M^4, P^2, P^4, P^6). A further parameter E_{ave} takes into account the kinetic energy of the electrons and their interactions with the nucleus. It shifts only the barycentre of the whole 4f configuration. So one can write [15]

$$H_{\text{free ion}} = \sum_k F^k f_k + \zeta_{4f} A_{so} + \alpha L(L+1) + \beta G(G_2) + \gamma G(R_7) + \sum_i T^i t_i + \sum_k P^k p_k + \sum_l M^l m_l \quad (2)$$

$i = 2, 3, 4, 6, 7, 8$; $k = 2, 4, 6$; $l = 0, 2, 4$.

Here f_k and A_{so} represent the angular part of the electrostatic and spin–orbit interaction respectively; L is the total orbital angular momentum; $G(G_2)$ and $G(R_7)$ are the Casimir operators for the groups G_2 and R_7; the t_i are the three-particle operators; and p_k and m_l represent the operators for the magnetic corrections.

The crystal-field Hamiltonian is given in the formalism of Wybourne [16] by

$$H_{\text{crystal field}} = \sum_{i=0}^{N} \sum_{k=0}^{\infty} \sum_{q=-k}^{k} B_q^k C_q^k(i). \quad (3)$$

Here $C_q^k(i)$ is a spherical operator of rank k, with components q. The B_q^k are the crystal-field parameters. N is the number of electrons, and i represents the ith electron. For f electrons $k \leqslant 6$. The non-zero conditions for the B_q^k are associated with the point-group site symmetry of the lanthanide ion. Only parameters with even k values are responsible for the crystal-field splitting. For a D_3 symmetry, the even part of $H_{\text{crystal field}}$ is expanded as

$$H_{D_3}^{\text{even}} = B_0^2 C_0^2 + B_0^4 C_0^4 + B_3^4 (C_{-3}^4 - C_3^4) + B_0^6 C_0^6 + B_3^6 (C_{-3}^6 - C_3^6) + B_6^6 (C_{-6}^6 + C_6^6). \quad (4)$$

The free-ion and crystal-field parameters are determined by optimizing a preliminary set of parameters in a least-squares fit to a set of experimentally determined crystal-field energy levels. The starting free-ion parameters are taken from $LaF_3:Eu^{3+}$ [17], and the starting crystal-field parameters are those from $YAl_3(BO_3)_4:Eu^{3+}$ [7]. J mixing is taken into account. First the crystal-field levels of $^7F_0$, $^7F_1$, $^7F_2$, $^5D_0$, $^5D_1$, $^5D_2$ and $^5L_6$ are used in the fit. The parameters that are allowed to vary are F^2, F^4, F^6, α, ζ_{4f}, B_q^4 and B_q^6. The repulsion parameters were in the first instance, however, held in the hydrogen-like ratio [13].

$$F^4 = 0.668F^2 \qquad F^6 = 0.494F^2.$$

The B_0^2 parameter was fixed at the value calculated from the splitting of the $^7F_1$ and $^5D_1$ levels. Indeed, the splitting of these levels is in the Russell-Saunders coupling scheme ($^7F_1$ and $^5D_1$ have more than 95% Russell–Saunders character) only determined by that parameter. Using the energy matrix in a Russell–Saunders basis, one finds that

$$\Delta E(^7F_1) = 0.30B_0^2 \text{ cm}^{-1} \qquad \Delta E(^5D_1) = 0.09B_0^2 \text{ cm}^{-1}.$$

Progressively more levels are introduced in the fitting procedure and more parameters were allowed to vary freely. The P^k parameters are always constrained to the ratio [17]

$$P^4 = 0.75P^2 \qquad P^6 = 0.50P^2.$$

P^2 is allowed to freely vary.

The root-mean-square deviation (RMS) σ for the final fit was 12.8 cm^{-1}. The optimized parameter set is given in table 3. The experimental and calculated energy levels for Eu^{3+} in $GdAl_3(BO_3)_4$ can be found in table 4. A total of 68 crystal-field levels are located and assigned.

Table 3. Free-ion and crystal-field parameters (in a D_3 symmetry) for Eu^{3+} in $GdAl_3(BO_3)_4$. The RMS for the last fit is 12.8 cm^{-1}. The values in parentheses are the errors on the parameters.

Parameter	Value (cm^{-1})	Parameter	Value (cm^{-1})
E_{ave}	63 443	ζ_{4f}	1328.9(1.2)
F^2	81 787(60)	M^0	2.20
F^4	59 534(71)	M^2	1.23
F^6	43 017(40)	M^4	0.84
α	21.912	P^2	319
β	−656	P^4	$0.75P^2$
γ	1377	P^6	$0.50P^2$
T^2	415(12)	B_0^2	530(40)
T^3	104(180)	B_0^4	−1164(50)
T^4	130(32)	B_3^4	−945(70)
T^6	−49(185)	B_0^6	688(29)
T^7	289(66)	B_3^6	110(51)
T^8	458(30)	B_6^6	−518(49)

6. Sensitivity analysis

The optimized set of free-ion and crystal-field parameters (table 3) are considered to give the best agreement between experimental and calculated energy levels. One can ask if this set is a unique one or if there are more sets possible. Not all parameters can be determined very accurately, because some can be varied over a rather large interval without causing great changes in the position of the calculated crystal-field levels. Other parameters only have an influence on a limited number of levels. The influence of a +10% change of the optimized free-ion parameters on the position of the calculated free-ion levels is given in table 5. The free-ion levels were calculated by setting all crystal-field parameters equal to zero. Only one parameter is changed during a single calculation. From table 5 it can be deduced which levels are sensitive for which parameters. A small change of such a sensitive parameter will cause a great change of the calculated energy levels. Parameters that show a great sensitivity can be determined accurately. One can draw the following conclusions:

(i) The electron repulsion parameters F^k have little influence on the ^7F multiplet, but the ^5D and ^5L multiplets are greatly influenced. A +10% change of F^2 causes a shift of ^7F and ^5D, which is opposite to the shift caused by F^4 and F^6. The absolute value of the shift increases with increasing k value.

(ii) The spin–orbit coupling parameter ζ_{4f} has a small influence on the $^5D_1$ and $^5L_6$, but most other levels are very sensitive to it. This parameter can be determined very accurately.

(iii) The configuration-interaction parameters α, β and γ have only little influence on the levels, compared to the electron repulsion on spin–orbit coupling parameters. The $^5L_6$ level is, however, rather sensitive to the α parameter, because α is important for levels with high L value (e.g. ^5L_J, ^5G_J, ^5H_J). $^5L_6$ and ^5D_J are sensitive to β and γ, but ^5F_J is not.

(iv) The T^k parameters have a negligible effect on the lower energy levels (< 25 000 cm^{-1}). T^2 and T^4 have a distinct influence on ^3P_J, and T^6 and T^7 on ^5H_J.

(v) A change of M^k and P^k has no marked influence on the energy level calculation. They cannot be excluded from the calculation, because they are able to correct for minor deviations.

It is evident that parameters that have only an influence on levels that are not observed in the experiment cannot be determined. They must be held constant during the fitting

Table 4. Experimental and calculated energy levels for Eu^{3+} in $GdAl_3(BO_3)_4$. The levels are assigned in a D_3 symmetry.

$^{2S+1}L_J$	Symmetry label	E_{exp} (cm^{-1})	E_{calc} (cm^{-1})	$^{2S+1}L_J$	Symmetry label	E_{exp} (cm^{-1})	E_{calc} (cm^{-1})
$^7F_0$	Γ_1	0	0	$^5G_{3,4,5,6}$	Γ_1	—	26525
					Γ_1	—	26557
$^7F_1$	Γ_3	331	334		Γ_3	26544	26544
	Γ_2	461	461		Γ_3	26583	26566
					Γ_2	26622	26609
$^7F_2$	Γ_3^a	940	932		Γ_3	26650	26634
	Γ_3^b	1061	1060		Γ_1	—	26635
	Γ_1	—	1195		Γ_2	—	26645
					Γ_1	—	26695
$^7F_3$–$^7F_6$		not observed in absorption			Γ_3	26717	26715
					Γ_2	—	26764
					Γ_1	—	26772
$^5D_0$	Γ_1	17245	17247		Γ_1	—	26779
					Γ_2	—	26797
$^5D_1$	Γ_3	19000	18991		Γ_3	26805	26800
	Γ_2	19030	19030		Γ_3	26834	26842
$^5D_2$	Γ_1	21442	21458	$^5D_4$	Γ_3^a	27574	27580
	Γ_3^a	21461	21461		Γ_1^a	—	27582
	Γ_3^b	21531	21513		Γ_3^b	27582	27598
					Γ_2	27591	27596
$^5D_3$	Γ_3^a	24327	24342		Γ_1^b	27655	27610
	Γ_3^b	24351	24356		Γ_3^c	27660	27672
	Γ_2^a	24357	24358	$^5H_{3,4,5,6,7}$	Γ_3	30668	30680
	Γ_2^b	24406	24388		Γ_2	30712	30699
	Γ_1	24420	24396		Γ_3	—	30760
					Γ_1	—	30781
$^5L_6$	Γ_1^a	—	24883		Γ_3	—	30803
	Γ_2^a	24903	24909		Γ_2	30824	30797
	Γ_3^a	24974	24978		Γ_1	—	30846
	Γ_1^b	24975	24988		Γ_3	30865	30860
	Γ_3^b	25052	25041		Γ_2	30973	30972
	Γ_1^c	—	25236		Γ_2	31012	31011
	Γ_2^b	25231	25237		Γ_1	—	31028
	Γ_3^c	25296	25327		Γ_3	—	31065
	Γ_3^d	25367	25360		Γ_3	—	31077
					Γ_1	—	31069
$^5L_7$, $^5G_2$	Γ_3	25956	25943		Γ_3	31103	31115
	Γ_2	26025	26041		Γ_3	31155	31159
	Γ_3	26051	26048		Γ_2	31156	31138
	Γ_1	—	26068		Γ_2	31190	31190
	Γ_3	26093	26087		Γ_3	—	31182
	Γ_2	26179	26183		Γ_3	—	31249
	Γ_3	26227	26225		Γ_3	31288	31295
	Γ_3	26272	26260		Γ_1	—	31299
	Γ_1	—	26277		Γ_3	31327	31337
	Γ_2	26288	26298		Γ_1	—	31329
	Γ_3	—	26309		Γ_2	31332	31333
	Γ_3	26332	26357		Γ_3	—	31357
	Γ_1	—	26383		Γ_3	31406	31409
					Γ_1	—	31412
$^5G_{3,4,5,6}$	Γ_1	—	26317		Γ_2	31400	31413
	Γ_2	26433	26431		Γ_3	31537	31525
	Γ_3	26435	26430		Γ_1	—	31535
	Γ_3	26455	26458		Γ_1	—	31542
	Γ_2	26465	26476		Γ_3	—	31550
	Γ_3	26484	26499		Γ_3	—	31569
	Γ_2	26513	26521		Γ_2	31620	31586
	Γ_3	26517	26523				

Table 5. Influence of a +10% change of the free-ion parameters on the calculated free-ion levels. The crystal-field parameters were set equal to zero. All values are expressed in cm^{-1}. Only one parameter was changed at a time.

ΔE	$^7F_1$	$^7F_2$	$^7F_3$	$^7F_4$	$^7F_5$	$^7F_6$	$^5D_0$	$^5D_1$	$^5D_2$	$^5D_3$	$^5D_4$	$^5L_6$
F^2	5.11	12.62	19.72	24.64	26.29	23.42	−267.21	−282.97	−284.64	−266.92	−208.48	409.84
F^4	−10.68	−23.10	−31.46	−33.95	−31.24	−24.64	994.95	1014.09	1030.16	1026.24	993.02	870.92
F^6	−18.92	−42.44	−61.12	−70.15	−66.51	−47.42	1277.46	1181.57	1139.89	1140.07	1181.74	975.29
ζ_{4f}	71.22	174.49	285.09	391.26	487.47	569.89	−325.18	−38.43	245.47	502.57	749.45	78.52
α	0.15	0.35	0.55	0.74	0.95	1.22	−10.00	−9.52	−9.22	−8.93	−8.16	97.84
β	0.75	1.63	2.25	2.47	2.25	1.63	−55.49	−53.54	−52.86	−53.19	−54.17	−69.54
γ	−1.72	−3.71	−5.09	−5.53	−4.97	−3.42	135.10	131.28	130.33	131.53	133.48	171.54
T^2	0.79	1.79	2.61	3.03	2.89	2.05	−46.39	−45.07	−44.54	−44.94	−45.86	−31.06
T^3	0.00	−0.01	−0.01	−0.01	−0.01	0.00	−0.03	0.03	0.08	0.09	0.08	−0.14
T^4	0.04	0.10	0.15	0.20	0.23	0.25	−2.67	−2.09	−1.70	−1.42	−1.25	−0.39
T^6	−0.02	−0.04	−0.07	−0.08	−0.09	−0.06	−0.25	−0.50	−0.79	−0.50	−0.12	−1.96
T^7	0.04	0.08	0.11	0.13	0.12	0.09	−2.26	−2.49	−2.62	−3.06	−3.11	−0.63
T^8	−0.23	−0.55	−0.84	−1.03	−1.05	−0.84	14.37	16.58	17.91	18.54	17.85	4.58
M^0	−1.24	−3.81	−7.76	−13.10	−19.88	−28.14	−8.49	−9.19	−11.56	−15.58	−20.88	7.84
M^2	−0.05	−0.07	−0.05	0.03	0.12	0.13	1.40	0.85	0.30	−0.27	0.71	−0.31
M^4	−0.02	−0.04	−0.04	−0.04	−0.04	−0.10	1.12	0.65	0.18	−0.29	−0.73	0.03
P^2	0.37	1.13	2.32	4.02	6.30	9.29	1.07	1.97	3.30	5.14	7.27	0.95
P^4	0.11	0.35	0.74	1.28	1.97	2.78	0.71	0.87	1.14	1.56	2.11	−0.92
P^6	0.01	0.04	0.09	0.17	0.28	0.45	0.76	0.47	0.26	0.10	−0.05	−0.20

procedure and are taken from parameter sets for the same ion in other matrices or can be found by extrapolation from parameter sets for other ions.

The sensitivity analysis can be extended to the crystal-field parameters. J mixing is applied in the calculations. Because of this J mixing, the free-ion levels (all crystal-field parameters set equal to zero) and the barycentres of the crystal-field levels do not coincide (table 6). J mixing has a great influence on the composition of the wavefunctions, and thus on the intensity of the transitions (see further). This was also noticed by Porcher and Caro [18] for Eu^{3+} in KY_3F_{10}. Because of the great number of crystal-field levels, only the influence of the parameters on ^5D_J and $^5L_6$ is considered.

Table 6. The calculated free-ion levels (all crystal-field parameters are set equal to zero) are not the same as the calculated barycentres of the crystal-field levels, when J mixing is taken into account. This is illustrated for the ^7F_J, ^5D_J and $^5L_6$ levels of Eu^{3+}. All values are expressed in cm^{-1}.

$^{2S+1}L_J$	Free-ion level	Barycentre	ΔE
$^7F_1$	379	371	8
$^7F_2$	1043	1014	29
$^7F_3$	1898	1850	48
$^7F_4$	2875	2861	14
$^7F_5$	3924	3962	−38
$^7F_6$	5012	5045	−33
$^5D_0$	17260	17229	31
$^5D_1$	19011	18984	27
$^5D_2$	21486	21441	45
$^5D_3$	24376	24265	111
$^5D_4$	27620	27557	63
$^5L_6$	25140	25052	88

The splitting of the $^5D_1$ is very sensitive to the B_0^2 parameter. The sign determines the relative position of the Γ_2 and Γ_3 levels. The magnitude of the parameter is proportional to the magnitude of the crystal-field splitting (as mentioned above). The B_0^2 parameter determines further the relative position of Γ_1 and Γ_2 in $^5D_3$ and of the Γ_3 levels in $^5L_6$. The B_0^4 parameter is important for the splitting of the $^5D_2$ level. The position of Γ_1 relative to the two Γ_3 levels is only determined by this parameter. The B_3^4 has a distinct influence on the magnitude of the crystal-field splitting of $^5D_2$. The B_0^6 parameter can be determined accurately using the $^5D_4$ crystal-field levels. The parameter has only a global influence on the $^5D_1$, $^5D_2$ and $^5D_3$ levels. This is also to a lesser extent true for the B_3^6 and B_6^6 parameters. The crystal-field splitting of levels with low J values is to a minor degree influenced by B_q^k parameters with high k values. All the B_q^k parameters are responsible for the splitting of the $^5L_6$ term.

7. Intensity parameters

The intensity of the 4f–4f transitions is measured in terms of the dipole strength, which can be deduced from the spectra by integrating the absorption peaks:

$$D_{\text{exp}} = \frac{1}{3 \times 108.9} \frac{g_i}{X_i(T)} \int \frac{\varepsilon(\bar{\nu})}{\bar{\nu}} \, d\bar{\nu} \tag{5}$$

where g_i is the degeneracy of the crystal-field ground level i, $X_i(T)$ is the fractional population of the crystal-field ground level i at temperature T, $\varepsilon(\bar{\nu})$ is the molar absorptivity at wavenumber $\bar{\nu}$ and D_{exp} is the experimental dipole strength (Debye^2). D_{exp} contains both ED and MD contributions:

$$D_{\text{exp}} = \chi_{\text{MD}} D_{\text{exp}}^{\text{MD}} + \chi_{\text{ED}} D_{\text{exp}}^{\text{ED}}. \tag{6}$$

χ_{MD} and χ_{ED} are corrections for medium effects:

$$\chi_{\text{MD}} = n \tag{7}$$

$$\chi_{\text{ED}} = (n^2+2)^2/9n \tag{8}$$

where n is the refractive index. For uniaxial crystals with a small birefringence, the two main refractive indices can be replaced by a mean value. For $GdAl_3(BO_3)_3$, $\chi_{\text{MD}} \simeq 1.75$ and $\chi_{\text{ED}} \simeq 1.63$. The dipole strengths are determined for the orthoaxial σ and π spectra.

The dipole strength D is also defined as the absolute square of the matrix element between the dipole operator and the crystal-field wavefunctions $\Psi_{\tau SLJM}$ and $\Psi_{\tau' SL'J'M'}$ of both the ground level and the excited level:

$$D = |\langle \Psi_{\tau SLJM} | O | \Psi_{\tau' SL'J'M'} \rangle|^2 \tag{9}$$

where O represents the MD operator μ_ρ or the ED operator m_ρ.

The total calculated dipole strength is given by

$$D_{\text{calc}} = \chi_{\text{MD}} D_{\text{calc}}^{\text{MD}} + \chi_{\text{ED}} D_{\text{calc}}^{\text{ED}}. \tag{10}$$

The dipole strength of a MD transition can be calculated using the crystal-field wavefunctions which are generated by the energy parameters. Only a limited number of transitions have a predominant MD nature: $^5D_1 \leftarrow {}^7F_0$, $^5D_0 \leftarrow {}^7F_1$ and $^5D_2 \leftarrow {}^7F_1$.

However, for the calculation of the dipole strength of an ED transition, an additional set of parameters is required, the $B_{\lambda kq}$ intensity parameters:

$$\begin{aligned}\langle \Psi_{\tau SLJM} | m_\rho | \Psi_{\tau' SL'J'M'} \rangle &= -|e| \sum_{\lambda kq} B_{\lambda kq} (2\lambda+1) \begin{pmatrix} 1 & \lambda & k \\ \rho & -q-\rho & q \end{pmatrix} (-1)^{q+\rho} \langle \Psi_{\tau SLJM} | U_{q+\rho}^{\lambda} | \Psi_{\tau' SL'J'M'} \rangle \\ &= -|e| \sum_{\lambda kq} a_{\lambda kq}^{\rho} B_{\lambda kq}. \end{aligned} \tag{11}$$

An explanation of the intensity model used can be found in Reid and Richardson [9–11]. These authors use, however, A_{tp}^{λ} parameters:

$$A_{tp}^{\lambda} = -B_{\lambda kq}(2\lambda+1)/(2k+1)^{1/2} \qquad t = k \text{ and } p = q. \tag{12}$$

The $B_{\lambda kq}$ parameters are more suitable for crystal-field transitions than the traditional Judd–Ofelt parameters [19, 20], because the latter describe the intensity between whole spin–orbit coupling bands. The site symmetry of the lanthanide ion places certain restrictions on the permissible pairs of (k, q) for each λ. In a D_3 symmetry, one has to consider 21 different $B_{\lambda kq}$ intensity parameters. The allowed (λ, k, q) combinations are: (2,2,0), (2,3,±3),

(4,3,±3), (4,4,0), (4,4,±3), (4,5,±3), (6,5,±3), (6,6,0), (6,6,±3), (6,6,±6), (6,7,±3) and (6,7,±6). The number of parameters can be reduced to 12 using the relationship

$$B_{\lambda kq} = (-1)^{k+q+1} B^*_{\lambda k,-q}. \tag{13}$$

The intensity parameters are determined by fitting the calculated D^{ED}_{calc} against the experimental D^{ED}_{exp} (which is determined from D_{exp} minus the calculated MD contributions). Not every $B_{\lambda kq}$ has an equal contribution to the intensity of an ED transition. In fact, the following selection rule is applicable:

$$|\Delta J| \leqslant \lambda \leqslant J + J'. \tag{14}$$

The $^5D_2 \leftarrow {}^7F_0$ and $^5D_1 \leftarrow {}^7F_1$ transitions can be used for the determination of the B_{220} and B_{223} parameters. Transitions to the $^5L_6$ level are suitable for fitting the six B_{6xx} parameters. In theory only the B_{4xx} parameters are needed to calculate the intensity of transitions to the $^5D_4$ multiplet, but the B_{6xx} parameters have also a major contribution. Indeed, the wavefunctions of the $^5D_4$ crystal-field levels have a significant $^5G_6$ character. After the preliminary determination of the $B_{\lambda kq}$ parameters, the parameter set is refined by taking the other transitions into account.

The $B_{\lambda kq}$ parameters are given in table 7. There is an uncertainty about the sign of the intensity parameters. This has no effect on the calculated dipole strengths, but it may have an effect on other calculated parameters such as the rotatory strength and MCD parameters [21]. The calculated and experimental dipole strengths are summarized in table 8.

Table 7. $B_{\lambda kq}$ intensity parameters for Eu^{3+} in $GdAl_3(BO_3)_4$.

Parameter	Value (cm)
B_{220}	61×10^{-12}i
B_{233}	227×10^{-12}i
B_{433}	104×10^{-12}i
B_{440}	-216×10^{-12}i
B_{443}	46×10^{-12}i
B_{453}	-99×10^{-12}i
B_{653}	30×10^{-12}i
B_{660}	70×10^{-12}i
B_{663}	2×10^{-12}i
B_{666}	-5×10^{-12}i
B_{673}	111×10^{-12}i
B_{676}	-64×10^{-12}i

8. Conclusions

A detailed analysis of the absorption spectrum of Eu^{3+}-doped $GdAl_3(BO_3)_4$ is given. The energy levels are parametrized in terms of 20 free-ion and six crystal-field parameters. The spectral intensities are simulated using a set of $B_{\lambda kq}$ intensity parameters. Anisotropic ligand polarization is taken into account. This model gives a fairly good description of the f–f transition probabilities. The present work provides the first complete set of energy and intensity parameters for lanthanide ions surrounded by borate groups. The crystal-field

Table 8. Experimental and calculated dipole strengths of 4f–4f transitions for Eu^{3+} in $CdAl_3(BO_3)_4$. All values are expressed in 10^{-8} Debye^2. The ED intensities are calculated using the $B_{\lambda kq}$ parameters from table 7.

Transition	Symmetry label	Polarization	Mechanism	D_{exp}	D_{calc}
$^5D_0 \leftarrow {}^7F_1$	$\Gamma_1 \leftarrow \Gamma_2$	σ	MD	557	536
	$\Gamma_1 \leftarrow \Gamma_3$	π	MD	471	540
$^5D_1 \leftarrow {}^7F_0$	$\Gamma_3 \leftarrow \Gamma_1$	π	MD	105	123
	$\Gamma_2 \leftarrow \Gamma_1$	σ	MD	67	68
$^5D_1 \leftarrow {}^7F_1$	$\Gamma_3 \leftarrow \Gamma_2$	σ	ED	189	272
	$\Gamma_2 \leftarrow \Gamma_2$	—	—	—	0.0
	$\Gamma_3 \leftarrow \Gamma_3$	σ	ED	3684	3583
	$\Gamma_3 \leftarrow \Gamma_3$	π	—	—	0.0
	$\Gamma_2 \leftarrow \Gamma_3$	σ	ED	181	257
$^5D_2 \leftarrow {}^7F_0$	$\Gamma_1 \leftarrow \Gamma_1$	—	—	—	0.0
	$\Gamma_3^a \leftarrow \Gamma_1$	σ	ED	641	846
	$\Gamma_3^b \leftarrow \Gamma_1$	σ	ED	631	637
$^5D_2 \leftarrow {}^7F_1$	$\Gamma_1 \leftarrow \Gamma_2$	—	—	—	3
	$\Gamma_3^a \leftarrow \Gamma_2$	σ	ED	504	285
	$\Gamma_3^b \leftarrow \Gamma_2$	—	ED	—	0.0
	$\Gamma_1 \leftarrow \Gamma_3$	—	—	—	0.0
	$\Gamma_3^a \leftarrow \Gamma_3$	σ	ED	62	5
	$\Gamma_3^b \leftarrow \Gamma_3$	σ	ED	75	103
$^5D_3 \leftarrow {}^7F_0$	$\Gamma_2^a \leftarrow \Gamma_1$	π	ED	2	2
	$\Gamma_2^b \leftarrow \Gamma_1$	π	ED	5	0.4
	$\Gamma_1 \leftarrow \Gamma_1$	—	—	—	0.0
	$\Gamma_2^b \leftarrow \Gamma_1$	—	—	—	2
	$\Gamma_3^a \leftarrow \Gamma_1$	σ	ED	7	0.5
$^5L_6 \leftarrow {}^7F_0$	$\Gamma_1^a \leftarrow \Gamma_1$	π	ED	—	0.0
	$\Gamma_2^a \leftarrow \Gamma_1$	π	ED	121	153
	$\Gamma_1^b \leftarrow \Gamma_1$	π	ED	—	0.0
	$\Gamma_1^c \leftarrow \Gamma_1$	π	ED	—	0.0
	$\Gamma_2^b \leftarrow \Gamma_1$	π	ED	3239	3601
	$\Gamma_3^a \leftarrow \Gamma_1$	σ	ED	258	466
	$\Gamma_3^b \leftarrow \Gamma_1$	σ	ED	2794	2818
	$\Gamma_3^c \leftarrow \Gamma_1$	σ	ED	—	197
	$\Gamma_3^d \leftarrow \Gamma_1$	σ	ED	5415	5183
$^5D_4 \leftarrow {}^7F_0$	$\Gamma_3^a \leftarrow \Gamma_1$	σ	ED	776	773
	$\Gamma_3^b \leftarrow \Gamma_1$	σ	ED	680	681
	$\Gamma_3^c \leftarrow \Gamma_1$	σ	ED	262	264
	$\Gamma_2 \leftarrow \Gamma_1$	π	ED	466	463
	$\Gamma_1^b \leftarrow \Gamma_1$	—	ED	238[a]	0.0
	$\Gamma_1^a \leftarrow \Gamma_1$	—	ED	—	0.0

[a] A $\Gamma_1 \rightarrow \Gamma_1$ transition is forbidden by the selection rules in D_3 symmetry. Its presence is probably due to depolarization effects.

splittings are comparable to those found in the corresponding Y^{3+} compound [7]. Although the crystal-field felt by the Eu^{3+} in other matrices is expected to be different (compare with

EuODA [13] and $LiYF_4:Eu^{3+}$ [14]), there are also small changes in the free-ion parameters. This may be due, for example, to nephelauxetic effects [22]. The influence of a parameter change on the calculated energy levels is discussed. It is worth noting that some parameters have only a distinct influence on particular levels. A change of the repulsion parameters F^k has little influence on the ^7F levels, whereas ^5D and ^5L are greatly influenced. The spin–orbit coupling parameter ζ_{4f} has a strong influence on most levels, except $^5D_1$ and $^5L_6$. The $^5L_6$ is, on the other hand, rather sensitive to α. This is expected for a term with a high orbital angular momentum L. ^5D_J and $^5L_6$ are sensitive to β and γ, but ^7F_J is not. T^2 and T^4 have a distinct influence on ^3P_J, T^6 and T^7 on ^5H_J. Not all crystal-field parameters are responsible for the splitting of a particular J level. So the splitting of $^5D_1$ and $^7F_1$ is described in a good approximation only by the B_0^2 parameter.

Knowledge of this sensitivity is a valuable tool in the fitting procedure. It serves to decide which parameters may be varied freely and which may not. The calculated positions of those sensitive levels are a good check for the reliability of a parameter.

Acknowledgments

We thank H Crosswhite for developing the programs that are used in simulating the energy level scheme. KB (aspirant NFWO) thanks the NFWO (Belgium) for financial support. The Belgian Government is also gratefully acknowledged (Programmatie van het Wetenschapsbeleid).

References

[1] Kuroda R, Mason S F and Rosini C 1981 *J. Chem. Soc. Faraday Trans.* 2 **77** 2125
[2] Lagerwey A A F and Blasse G 1975 *Chem. Phys. Lett.* **31** 27
[3] Peacock R D 1975 *Chem. Phys. Lett.* **35** 420
[4] Kellendonk F and Blasse G 1981 *J. Chem. Phys.* **75** 561
[5] Görller-Walrand C and Vandevelde P 1985 *Bull. Soc. Chim. Belg.* **94** 873
[6] Görller-Walrand C and Vandevelde P 1985 *Chem. Phys. Lett.* **122** 276
[7] Görller-Walrand C, Vandevelde P, Hendrickx I, Porcher P, Krupa J C and King G S D 1988 *Inorg. Chim. Acta* **143** 259
[8] Mason S F, Peacock R D and Stewart B 1975 *Mol. Phys.* **30** 1829
[9] Reid M F and Richardson F S 1983 *Chem. Phys. Lett.* **95** 501
[10] Reid M F and Richardson F S 1983 *J. Chem. Phys.* **79** 5735
[11] Reid M F and Richardson F S 1984 *J. Phys. Chem.* **88** 3579
[12] Koster G F, Dimmock J O, Wheeler R G and Statz H 1963 *Properties of the Thirty-two Point Groups* (Cambridge, MA: MIT)
[13] Berry M T, Schwieters C and Richardson F S 1988 *Chem. Phys.* **122** 105
[14] Görller-Walrand C, Binnemans K and Fluyt L 1993 *J. Phys.: Condens. Matter* **5** 8359
[15] Crosswhite H M and Crosswhite H 1984 *J. Opt. Soc. Am.* B **1** 246
[16] Wybourne B G 1965 *Spectroscopic Properties of Rare Earths* (New York: Wiley)
[17] Carnall W T, Goodman G L, Rajnak K and Rana R S 1988 A systematic analysis of the spectra of the lanthanides doped into single crystal LaF_3 *Technical Report* Argonne National Laboratory
[18] Porcher P and Caro P 1980 *J. Lumin.* **21** 207
[19] Judd B R 1962 *Phys. Rev.* **127** 750
[20] Ofelt G S 1962 *J. Chem. Phys.* **37** 511
[21] Görller-Walrand C, Verhoeven P, Fluyt L, D'Olieslager J and Binnemans K 1994 *J. Chem. Phys.* **100** 815
[22] Caro P, Beaury O and Antic E 1976 *J. Physique* **37** 671